

Information and Computing Sciences  
Faculty of Science, Utrecht University



## Experimentation Project

# Physical Fatigue Assessment for Virtual Character Animation

*Author:*  
Elena Alexandra Ursu

*Supervisor:*  
Dr. Nicolas Pronost

December 12, 2012

### **Abstract**

This report presents an experimentation on a fatigue model from literature [Ma et al., 2009]. The model is based on the way humans perceive muscle fatigue on their own bodies and is correlated, from a biological point of view, to the muscle motor-unit mechanism. Thoroughly validated for static cases, the model is considered promising for dynamic situations as well. This report analyzes and compares the fatigue in three different animations taken from an online motion capture database and compares the rate at which the motions inflict fatigue on the performers. The numerical results are correlated with the intuitive expectations of the fatigue outcome of the three motions.

# Contents

<b>1</b>	<b>Introduction</b>	<b>3</b>
<b>2</b>	<b>Method description</b>	<b>4</b>
2.1	Dynamic fatigue model . . . . .	4
2.2	Extension to the joint level . . . . .	5
2.3	Static and dynamic cases . . . . .	5
<b>3</b>	<b>Implementation details</b>	<b>7</b>
3.1	Motion dataset . . . . .	7
3.2	Scaling the inertial properties . . . . .	8
3.3	Fatigue . . . . .	9
<b>4</b>	<b>Results</b>	<b>11</b>
<b>5</b>	<b>Conclusions</b>	<b>16</b>
<b>A</b>	<b>BVH file format</b>	<b>18</b>
<b>B</b>	<b>BVH file template</b>	<b>18</b>
<b>C</b>	<b>GEAR Inverse Dynamics</b>	<b>19</b>
<b>D</b>	<b>Application description</b>	<b>20</b>

# 1 Introduction

This report presents an experimentation on a fatigue model from literature [Ma et al., 2009] that was developed with the scope of analyzing musculoskeletal disorder (MSD) risk in physical labor. The authors worked extensively on industrial applications, and were able to determine which is the best pose for the worker to feel the least fatigue and provide guidelines for the work-rest schedules. Another possible application, more interesting for computer animation, would be to assess fatigue during a motion and to alter the motion correspondingly. This would enhance realism, as humans get tired in time, which is not just an internal feeling, but also reflects in their posture and activity.

The fatigue model introduced in [Ma et al., 2009] was formulated at muscle level, then extended at joint level in [Ma et al., 2010]. Intuitively, the model is based on the way humans perceive muscle fatigue on their own bodies. From a biological point of view, the model is correlated to the muscle motor-unit mechanism.

Thoroughly validated for static cases (when the load exerted on a muscle is constant in time), the model is considered promising for dynamic situations as well. Based on this statement, this report analyzes and compares the fatigue evaluation for three motions taken from an online motion capture database.

The joint level fatigue model is based on joint torques obtained through inverse dynamics. Another problem is determining the load of each muscle that drives the motion. A solution to this problem is the CMC tool from OpenSim [CMC], which uses proportional-derivative control and static optimization to calculate muscle excitations that drive the character towards its imposed trajectory. This report will explain the joint level fatigue model applied on motions from the CMU Graphics Lab Motion Capture Database [CMU], with the aid of an inverse dynamics library called GEAR, released at [Kim, a].

The structure of the report is as follows. In chapter [Method Description](#), the dynamic muscle fatigue model is presented in detail, as well as the extension to joint level. The mathematical background to derive the equations is also explained. Then, the related work is briefly reviewed to obtain an insight into the difference between static and dynamic cases.

Chapter [Implementation details](#) presents all the resources that were put together to create the fatigue evaluation pipeline. Detailed explanations are given on the important parts, such as scaling the inertial parameters.

Chapter [Results](#) evaluates the fatigue in three different animations (see [Figure 1](#)) and compares the rate at which the motions inflict fatigue on the performers. The numerical results are correlated with the intuitive expectations of the fatigue outcome of the three motions.

Chapter [Conclusions](#) summarizes the achievements of this project, the points that can be improved, the advantages and drawbacks of the selected method, as well as the current direction that the authors of the method are exploring.

Finally, the [Appendix](#) gives additional information on the BVH motion capture file format used in this project, on the inverse dynamics algorithm implemented in the GEAR library and on the user instructions for the application.

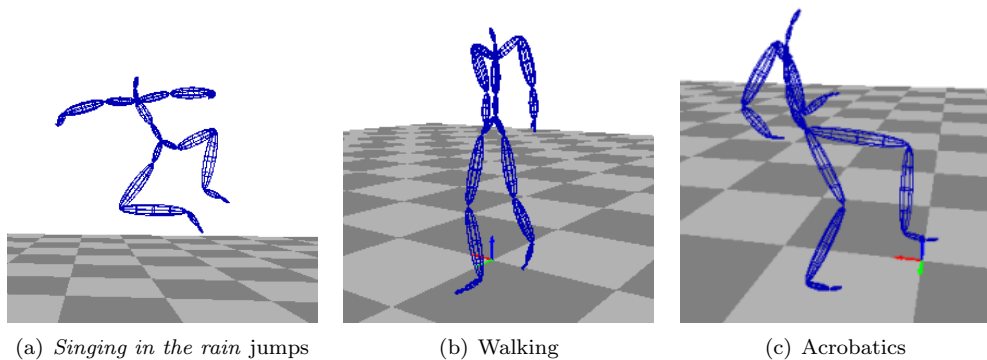


Figure 1: Stills of the motions analyzed in the [Results](#) chapter

## 2 Method description

### 2.1 Dynamic fatigue model

This section will describe in detail the dynamic fatigue model introduced by [Ma et al., 2009]. To understand the fatigue model, it is necessary to start from the fatigue index, as described in the paper. The fatigue index represents an evaluation of the muscle fatigue perceived by a person on their own body. Fatigue perception can be synthesized in the following points:

- a. Fatigue grows with the external load (the force exerted on the muscle along time) - the larger this load, the more fatigue people feel.
- b. Fatigue grows with the inverse of the muscle force capacity - the smaller the muscle capacity, the faster the muscle gets fatigued.
- c. Fatigue grows with time - the longer the physical task, the more fatigued the organism becomes.

Based on the these observations, the fatigue index  $U$  is given in equation (2.1).

$$\frac{dU(t)}{dt} = \frac{MVC}{F_{cem}(t)} \frac{F_{load}(t)}{F_{cem}(t)} \quad (2.1)$$

The explanation of the terms in (2.1) is the following:

- $U$  represents the fatigue index, in minutes.
- $F_{cem}$  represents the current exertable maximum force, or the current muscle capacity, in Newtons. Naturally, this force drops in time as the muscle becomes fatigued.
- $MVC$  stands for maximum voluntary contraction and represents the maximum capacity of muscle which is a personal factor and can be determined per individual and per muscle.
- $F_{load}$  is the force that the muscle needs to generate

Observing that  $F_{cem}(t)$  decreases with time due to  $F_{load}(t)$ , equation (2.2) gives the *dynamic fatigue model*:

$$\frac{dF_{cem}(t)}{dt} = -k \frac{F_{cem}(t)}{MVC} F_{load}(t) \quad (2.2)$$

The term  $k$  in (2.2) is called a *fatigue ratio* and is assigned a constant value of  $1min^{-1}$ . To be consistent with the paper, the equations will remain literal in the following demonstrations and the term  $k$  will be substituted with the actual value in the implementation. Thus, equation (2.2) can be rewritten as:

$$\frac{dF_{cem}(t)}{F_{cem}(t)} = \frac{-k}{MVC} F_{load}(t) dt \quad (2.3)$$

and solved as a separable differential equation.

$$\int \frac{dF_{cem}(t)}{F_{cem}(t)} = \int \frac{-k}{MVC} F_{load}(u) du \Rightarrow \quad (2.4)$$

$$\ln F_{cem}(t) = \int \frac{-k}{MVC} F_{load}(u) du + \ln |C|, C \in \mathbb{R}^* \Rightarrow |F_{cem}(t)| = e^{\int \frac{-k}{MVC} F_{load}(u) du + \ln |C|} \Rightarrow \quad (2.5)$$

$$F_{cem}(t) = e^{\int \frac{-k}{MVC} F_{load}(u) du + \ln |C|} \Rightarrow F_{cem}(t) = C e^{\int \frac{-k}{MVC} F_{load}(u) du} \quad (2.6)$$

To determine constant  $C$ ,

$$F_{cem}(0) = C \quad (2.7)$$

Knowing that at  $t = 0$ , the muscle capacity is maximum, we can write that

$$F_{cem}(0) = MVC \Rightarrow C = MVC \quad (2.8)$$

Now, from (2.6) and (2.8) we get the solution of the dynamic fatigue model,

$$F_{cem}(t) = MVC e^{\int \frac{-k}{MVC} F_{load}(u) du} \quad (2.9)$$

## 2.2 Extension to the joint level

Joints are moved by torques generated by their connected muscles. However, it is difficult to describe each muscle's contribution. Instead, it is accurate enough to calculate torques for each joint from inverse dynamics. For this reason, [Ma et al., 2010] extend the dynamic fatigue model to the joint level, with just a few simple substitutions:

- $MVC$  becomes the *maximum joint strength*  $\Gamma_{max}$
- $F_{load}$  becomes the *joint load torque*  $\Gamma_{load}$
- $F_{cem}$  becomes the *current joint strength with time*  $\Gamma_{cem}$

With these new parameters, equation (2.9) becomes:

$$\Gamma_{cem}(t) = \Gamma_{max} e^{\int \frac{-k}{\Gamma_{max}} \Gamma_{load}(u) du} \quad (2.10)$$

This equation gives the measure investigated in this report and represents the basis of this project's implementation (see Section 3.3).

## 2.3 Static and dynamic cases

**Static cases** The muscle fatigue model implemented in this project was extensively studied for *static* cases (where  $F_{load}(t)$  is constant). [Ma et al., 2009] derived the Maximum Endurance Time (MET - a measure related to static muscular work) model from their own dynamic model and found a good linear correlation with 24 other experimental static endurance models existent in literature. [Ma et al., 2010] evaluated the fatigue of a manual handling operation, namely a worker drilling holes around a fuselage circumference for the assembly of an airplane. The fatigue in the right arm was assessed leading to a posture analysis that gave valuable indications on the optimal position between shoulder and elbow during the task to minimize the stress and discomfort of the worker. Again, the external load was considered constant in time, and other influences such as vibration were neglected.

Moreover, the same situation was examined in [Ma et al., 2011a] to predict the endurance time for the drilling task. It was found that the shoulder joint played a key role at limiting the work time, due to the reduced endurance compared to the elbow. [Ma et al., 2011b] further analyzed the model and used mathematical regression to determine the fatigability (or fatigue resistance) of different muscle groups.

**Dynamic cases** [Ma et al., 2009] compared their model with three other dynamic models both qualitatively and quantitatively, where possible. The model introduced by [Freund and Takala, 2001] expressed the force production capacity  $S^0$  in relation to the upper limit of the muscle force  $S^l$  and to the muscle force  $S$  with the following formula:

$$\frac{dS^0}{du} = \alpha(S^l - S^0) - \beta S \quad (2.11)$$

where  $\alpha$  and  $\beta$  were fitted experimentally in a static endurance time test. Qualitatively, the same idea was used to describe the muscle fatigue mechanism both in [Ma et al., 2009]'s model and this model. Namely, both the muscle force production capacity  $S^0$  and the current exertable maximum force  $F_{cem}$  described the capacity of the muscle after performing a certain task.

Also from a qualitative point of view, the same trend expressed by equation (2.2) was found in the work of [Wexler et al., 1997]. To be more precise, the relationship between the maximum exertable force and time in both models showed that the larger the peak force, the faster the maximum exertable force declined and the muscle became fatigued more rapidly.

From a quantitative point of view, the fatigue model was compared with the work of [Liu et al., 2002]. Their model based on motor units pattern expressed the generated force in relationship to the activated motor units in the muscle. The mathematical formula of this model was simplified assuming no recovery during the physical task and maximum brain effort, leading to:

$$\frac{M_A(t)}{M_0} + \frac{M_{uc}(t)}{M_0} = e^{-Ft} \quad (2.12)$$

where the sum of the activated motor units  $M_A(t)$  and motor units at rest  $M_{uc}(t)$  normalized by the number of total available motor units  $M_0$  is an exponential function of time and  $F$ , called the *fatigue factor* (which determines the rate of fatigue of the motor units).

The same form can be reached in [Ma et al., 2009]’s model by assuming that, in equation (2.9),  $F(t) = \int_0^t \frac{F_{load}(u)}{MVC} du$  and  $F_{load} = constant$ , therefore  $\frac{F_{load}}{MVC} = Ct$  and  $F(t) = Ct$ , thus leading to:

$$\frac{F_{cem}}{MVC} = e^{-kCt} \quad (2.13)$$

It can now be seen that equations (2.12) and (2.13) have the same form. The experiments performed by [Liu et al., 2002] involved gripping a hand grip with maximum force. This is called *MVC condition* and expressed as  $\frac{F_{load}}{MVC} = 1$  in [Ma et al., 2009]’s model. Comparison between the experimental results of the active motor model and the dynamic model in maximum effort showed that the fitting curves were almost identical.

The earlier assumptions were made due to the fact that these were the only conditions under which the experimental results from [Liu et al., 2002] were provided. It is important to note that this is a sensitive issue of this project, namely the fact that the muscle fatigue model was only verified under the MVC condition. However, the statement in [Ma et al., 2011a] that the aforementioned validation suggested that the model was suitable for modeling muscle fatigue in dynamic cases, the simplicity of the model and the availability for implementation and experimentation with existent resources were the main reasons for which this model was chosen as a topic for this project.

### 3 Implementation details

This chapter presents the implementation steps made to calculate the joint level fatigue evaluation according to formula (2.10). The workflow is schematically shown in Figure 2 and described in detail in the remainder of this chapter.

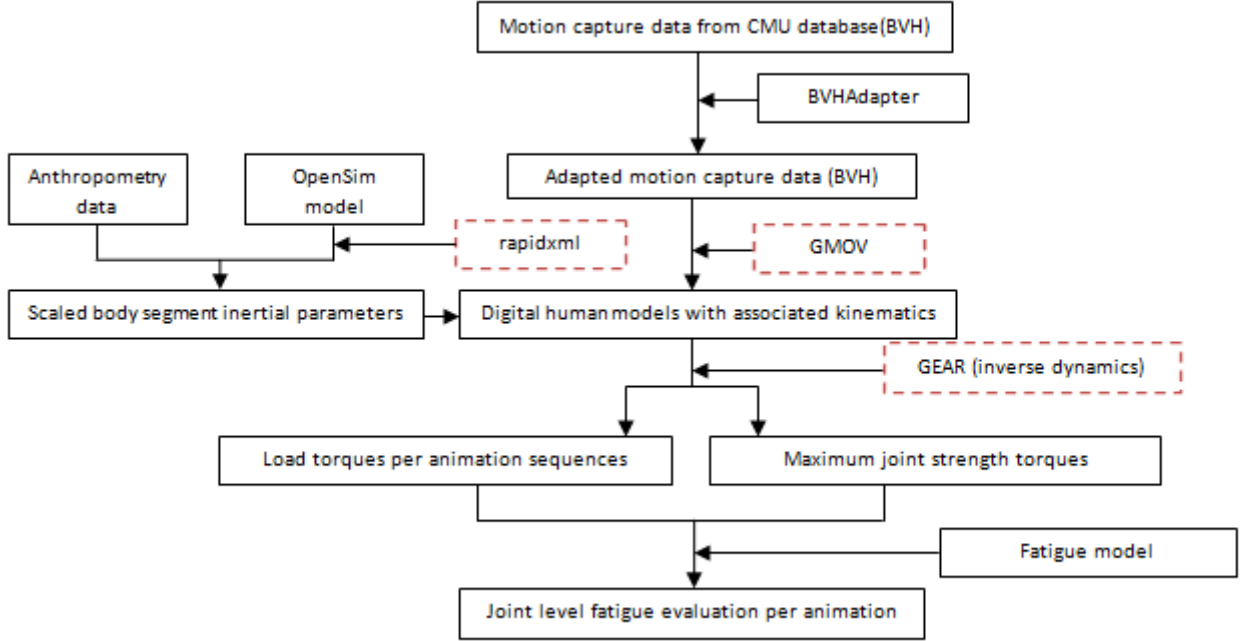


Figure 2: Fatigue evaluation for a single subject

The dashed boxes depict third-party libraries used in this project.

#### 3.1 Motion dataset

The motion capture sequences used in this project were retrieved from the BVH conversion of the Carnegie Mellon University motion capture dataset [CMU] released by Bruce Hahne in 2008 at [Hahne, 2008]. The dataset is conveniently organized in folders per subjects (a motion capture session performed by a single person) and contains a large variety of motions.

##### BVH file format

The BVH file format is a widely used format for storing motion capture data for character animation. It was developed by BioVision and consists of two parts. The first part describes the hierarchy of the skeleton. The second part, called the motion section, describes the channel data for each frame. These two parts are further explained in Appendix A, according to [Meredith and Maddock].

**Playing the animation** To parse the information in the BVH files, the GMOV application released by Junggon Kim at [Kim, b] was used in this project. The world space in GMOV and BVH is defined as a right handed coordinate system with the X axis pointing anteriorly to the character, the Y axis pointing vertically upward and the Z axis to the right of the character.

**Measure units** The offsets were scaled to meters by employing the formula given at [CMU]. The scaling was done by multiplying the values with  $(1.0/0.45)*2.54/100.0 = 0.056444$ .



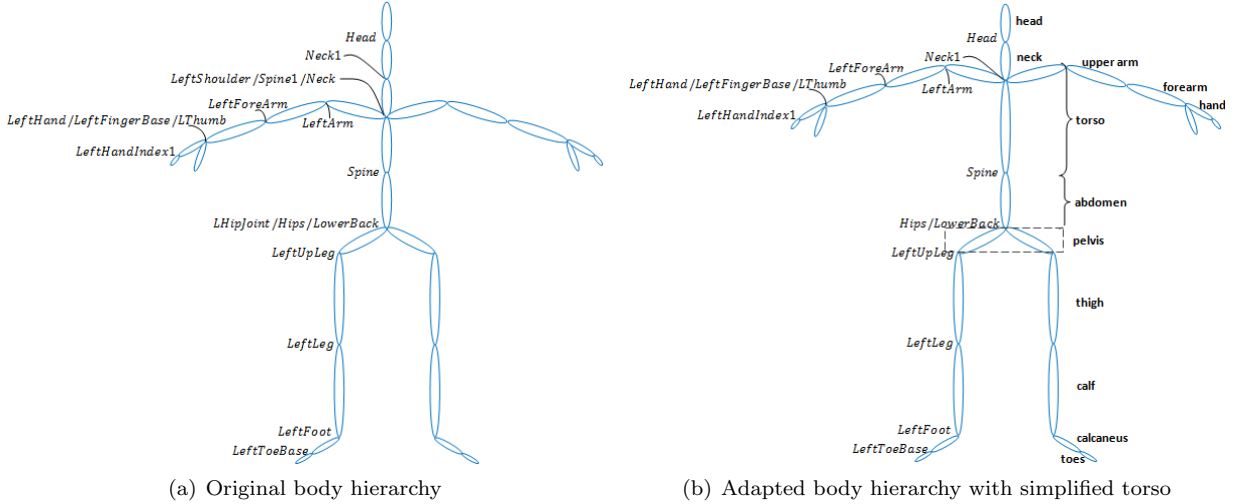


Figure 3: BVH body hierarchy

### 3.2 Scaling the inertial properties

Computing 3D inverse dynamics on character motion to obtain joint moments (see Section 3.3) requires that body segment inertial parameters are known. Each body segment in the virtual character was assigned mass and principle moments of inertia by scaling values from literature.

**BVH hierarchy** Fitting the body segmentation from the dataset provided by [Hahne, 2008] with the segmentation available in literature was a difficult task, and required the most effort in this project. Achieving a correspondence between the body segments from the BVH dataset and the literature segmentation was made possible through an adjustment of the body hierarchy (see Figure 3):

- five redundant joints (with null offsets) were removed: LHipJoint, RHipJoint, Neck, LeftShoulder, RightShoulder
- the Spine1 joint was removed and its offset was added to the Neck1 joint offset, in order to adjust the torso structure to correspond to the literature segmentation

A template BVH file was customized for this purpose, as listed in Appendix B. The channels of the removed joints were also removed from the motion section of the BVH files. The Neck1 joint channels remained intact.

The resulting hierarchy comprises 25 joints, accounting for 78 DOFs. The resulting motions closely follow the original ones, with noticeable yet negligible artifacts for the purpose of this project.

**Anthropometry data** Most of the body parts were scaled using the data from [Harry G. Armstrong Aerospace Medical Research Laboratory, 1988]. The process was not straightforward and required a number of fine-tunings. This was due to a number of reasons. First, a different body reference axis system was used, unlike the world coordinate system described above (see Section 3.1). Second, the neck, thorax, and pelvis principal axes in which the moments of inertia values were given were rotated from this reference position. Listing 1 shows the method that deals with the adjustments that amend these issues.

First, the method at line 5 from listing 1 transforms the moments of inertia from  $kg \cdot cm^2$  to  $kg \cdot m^2$ , and rotates them back to the body reference axis system. The rotation matrix is computed with the following formula:

$$R = \begin{bmatrix} \cos \theta + u_x^2(1 - \cos \theta) & u_x u_y(1 - \cos \theta) - u_z \sin \theta & u_x u_z(1 - \cos \theta) + u_y \sin \theta \\ u_y u_x(1 - \cos \theta) + u_z \sin \theta & \cos \theta + u_y^2(1 - \cos \theta) & u_y u_z(1 - \cos \theta) + u_x \sin \theta \\ u_z u_x(1 - \cos \theta) - u_y \sin \theta & u_z u_y(1 - \cos \theta) + u_x \sin \theta & \cos \theta + u_z^2(1 - \cos \theta) \end{bmatrix} \quad (3.1)$$

where  $(u_x, u_y, u_z)$  is the unit vector that gives the direction of the rotation axis and  $\theta$  is the rotation angle. Both  $\theta$  and the unit vector are parameters of the method.

```

1 void FatigueSystem::scaleFromAnthropometry(string startJoint, gReal length, gReal mass, gReal ixx
, gReal iyy, gReal izz, int ux, int uy, int uz, gReal theta)
3 {
    GBody* body = getBodySegmentByName(startJoint);
5     rotateMomentsOfInertia(theta, ux, uy, uz, ixx, iyy, izz);
    scaleMassFromAnthroToBVH(startJoint, mass, length, ixx, iyy, izz);
7     adjustToSCS(ixx, iyy, izz);
9     body->setMass(mass, ixx, iyy, izz, 0.0, 0.0, 0.0);
}

```

Listing 1: `scaleFromAnthropometry` method that scales body segments from [Harry G. Armstrong Aerospace Medical Research Laboratory, 1988] to the BVH character

Once the rotation matrix  $R$  is known, the inertia tensor  $I$  is transformed under rotation with the formula:

$$I' = RIR^T \quad (3.2)$$

The mass and inertia are then scaled (line 6 from listing 1) according to the ratio between the offsets from the BVH hierarchy and the corresponding segment lengths from [Harry G. Armstrong Aerospace Medical Research Laboratory, 1988]. The shoulders breadth ratio is used for the torso, while the hips breadth is used for the pelvis. The hands are scaled according to the forearms ratios and the head is scaled according to the torso ratio.

Lastly, the moments of inertia are changed from the body reference axis system to the world coordinate system (line 7 from listing 1) and the method from line 9 sets the inertial parameters for the current body.

**OpenSim model** The "3D Gait Model with Simple Arms" OpenSim model [osi] available from the OpenSim biomechanics simulation software from NIH National Center for Biomedical Computation [Ope] was used to scale the calcaneus and toes segments (comprising the foot). Parsing was done using RapidXml available at [Kalicinski, 2009].

Scaling the values from the model was done according to the offset vector of each segment in the BVH file and the location in parent of the ending joint of the corresponding segment in the OpenSim model. The ratio between the two lengths gave the mass scaling factor. The same ratio squared was used to scale the moments of inertia.

The calcanei and toes (see Figure 3) were scaled using the OpenSim model, while the remaining bodies were scaled using the data from [Harry G. Armstrong Aerospace Medical Research Laboratory, 1988]. In total, 19 body segments were scaled, corresponding to 21 joints (LeftFingerBase and RightFingerBase are offsetted with zeros from LeftHand and RightHand) accounting for 66 DOFs. The remaining segments (up to 25) were parts of the hands which moved little mass and were neglected for further computations.

### 3.3 Fatigue

The necessary values to calculate joint level fatigue, according to formula (2.10), are obtained through inverse dynamics, a method also used by [Ma et al., 2010]. Inverse rigid-body dynamics calculates torques based on the motion or kinematics of a body and its segments' inertial parameters (mass and moments of inertia). The motion is given in the dataset made of BVH files as described in Section 3.1, the inertial properties are attributed from literature as described in Section 3.2 and the inverse dynamics is performed using a free library released by Junggon Kim under the name GEAR [Kim, a]. The inverse dynamics algorithm is shortly described in Appendix C.

The maximum joint strength  $\Gamma_{max}$  represents the maximum exerted load torque for each DOF and is determined in a preprocessing phase. In this phase, all the animations for a subject are processed (load torques are computed at each frame through inverse dynamics), and each time a higher load torque has been exerted,  $\Gamma_{max}$  for that subject is updated accordingly. This is done separately for every available subject. The integral in formula (2.10) is calculated as a summation of (absolute values of) load torques in time.

At this moment, all the terms in (2.10) are known. The program prints the current joint strength  $\Gamma_{cem}$  at a flexible interval of time. To analyze the joint fatigue level, the measures related to *human status*, a concept introduced in [Ma et al., 2011a], are also presented in this report (see Results). These measures are:

- the normalized physical strength every  $n$  seconds  $\frac{\Gamma_{cem_i}}{\Gamma_{max}}$ , denoted as *current*
- the difference between the joint strength every  $n$  seconds  $\frac{\Gamma_{cem_i} - \Gamma_{cem_{i+1}}}{\Gamma_{max}}$ , denoted as *incremental*
- the difference between the joint strength and the maximum joint strength every  $n$  seconds  $\frac{\Gamma_{max} - \Gamma_{cem_i}}{\Gamma_{max}}$ , denoted as *relative*

In [Ma et al., 2011a], these measures are considered every 30 seconds (the necessary time for drilling a hole, as discussed in Section 2.3). In our experiments, the values are taken into consideration at a variable interval of time, depending on the characteristics of the analyzed motions (namely the length of the motion and the moments at which notable events occur).

## 4 Results

**Singing in the rain jumps** First, a "singing in the rain jump" sequence is analyzed. The motion consists of four jumps with the heels touching each other, with a few steps in between for momentum. The animation shows two consecutive jumps, then a brief phase in which the subject takes a few steps for momentum, then a third and a fourth jump which slightly decrease in amplitude (the performer gets tired). The difference between the joint strength every half second, *incremental*, is plotted in Figure 4. The first row shows the graphs for the left hip DOF corresponding to the rotation around the lateral axis and for the left knee DOF corresponding to the rotation around the vertical axis. The second row shows the graphs for the left shoulder DOF corresponding to the rotation around the anterior axis and for the left elbow DOF corresponding to the rotation around the vertical axis.

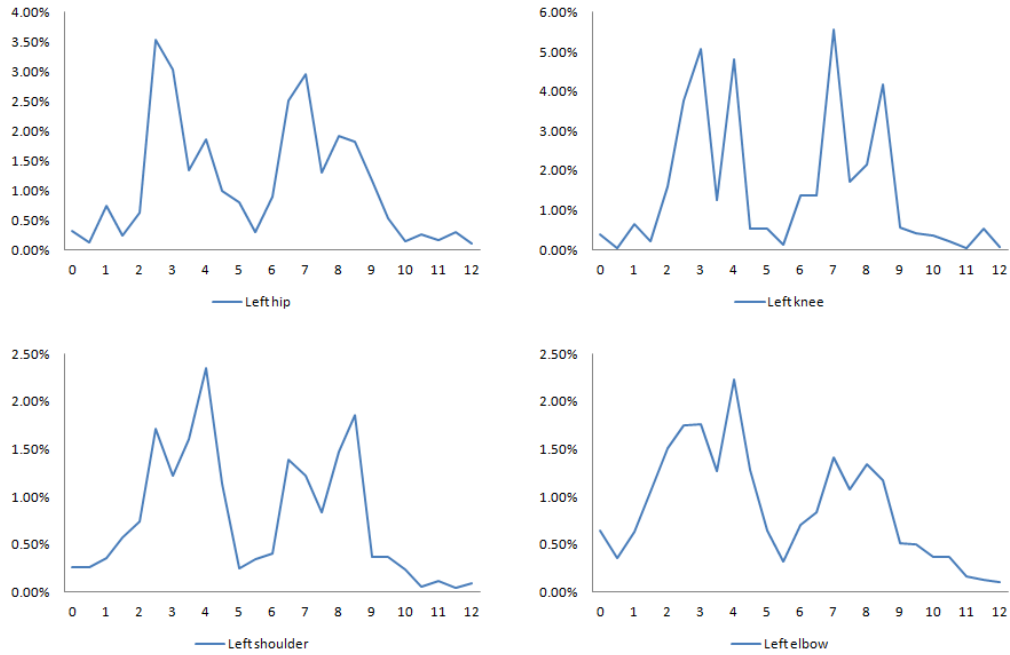


Figure 4: Difference between joint strength every half second for a "singing in the rain jump" sequence

The graphs show four peaks, corresponding to the jumps. The starting times (s) of the four jumps (the moment the first foot is lifted off the ground) are the following: 2.545, 3.848, 6.697, 8.061. The data can be interpreted as follows: as the jumps take more effort than the in-between phases, the decay rate of the current joint strength with time is higher at the respective moments. Unlike the values obtained in [Ma et al., 2011a] for the hole drilling task where the load is considered constant, the difference in joint strength does not decline steadily in time, but varies as the motion becomes more or less intense. The rest period between the two sets of consecutive jumps is also visible.

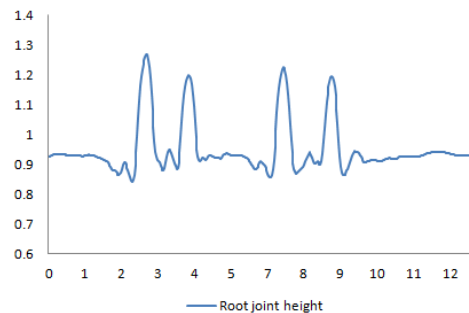


Figure 5: Height (Y coordinate) of the root joint every frame for a "singing in the rain jump" sequence

Figure 5 plots the height of the root joint every frame (at a frequency of 33 fps). It can be observed that the second and the fourth jumps decrease in altitude relatively to the first and third jump similarly to the

joint strength difference of the leg (mainly involved in the performance) joints (see Figure 4). On the other hand, the arm joints seem to compensate the less effort that goes into the leg by showing increased joint strength difference at the second and fourth jumps compared to the first and third jumps respectively.

Tables 1 and 2 give the normalized physical strength (*current*), the difference between the joint strength (*incremental*), and the difference between the joint strength and the maximum joint strength (*relative*), every second for the left leg joints and the left arm joints respectively.

Table 1: Normalized leg joints strength for the "singing in the rain" jumps

Time(s)	Left hip			Left knee		
	<i>current</i>	<i>incremental</i>	<i>relative</i>	<i>current</i>	<i>incremental</i>	<i>relative</i>
0.97	99.55%	0.44%	0.45%	99.50%	0.43%	0.50%
1.94	98.56%	1.00%	1.44%	98.64%	0.86%	1.36%
2.91	94.39%	4.16%	5.61%	93.26%	5.38%	6.74%
3.88	90.03%	4.36%	9.97%	86.94%	6.32%	13.06%
4.85	87.19%	2.85%	12.81%	81.58%	5.36%	18.42%
5.82	86.09%	1.10%	13.91%	80.92%	0.66%	19.08%
6.79	82.69%	3.40%	17.31%	78.18%	2.74%	21.82%
7.76	78.45%	4.25%	21.55%	70.90%	7.28%	29.10%
8.73	74.70%	3.74%	25.30%	64.59%	6.31%	35.41%
9.70	73.01%	1.69%	26.99%	63.62%	0.97%	36.38%
10.67	72.60%	0.41%	27.40%	63.07%	0.55%	36.93%
11.64	72.13%	0.47%	27.87%	62.49%	0.58%	37.51%
12.61	71.94%	0.19%	28.06%	62.40%	0.08%	37.60%

Table 2: Normalized arm joints strength for the "singing in the rain" jumps

Time(s)	Left shoulder			Left elbow		
	<i>current</i>	<i>incremental</i>	<i>relative</i>	<i>current</i>	<i>incremental</i>	<i>relative</i>
0.97	99.48%	0.51%	0.52%	98.99%	1.00%	1.01%
1.94	98.56%	0.92%	1.44%	97.30%	1.69%	2.70%
2.91	96.11%	2.45%	3.89%	94.04%	3.26%	5.96%
3.88	93.28%	2.83%	6.72%	91.00%	3.04%	9.00%
4.85	89.78%	3.50%	10.22%	87.48%	3.52%	12.52%
5.82	89.19%	0.59%	10.81%	86.52%	0.96%	13.48%
6.79	87.39%	1.79%	12.61%	84.97%	1.55%	15.03%
7.76	85.33%	2.07%	14.67%	82.48%	2.49%	17.52%
8.73	81.99%	3.33%	18.01%	79.95%	2.52%	20.05%
9.70	81.27%	0.73%	18.73%	78.94%	1.01%	21.06%
10.67	80.99%	0.28%	19.01%	78.21%	0.73%	21.79%
11.64	80.83%	0.15%	19.17%	77.92%	0.29%	22.08%
12.61	80.68%	0.15%	19.32%	77.77%	0.15%	22.23%

The first column shows how the physical strength declines in time. The middle column corresponds to the graphs in Figure 4 and was discussed previously. The last column shows that as the current joint strength with time  $\Gamma_{cem}$  decreases, the normalized difference between the maximum joint strength  $\Gamma_{max}$  and  $\Gamma_{cem}$  increases. The increase rate is higher around the jump times, when the subject performs more ample movements.

**Walking** Next, a walking sequence is analyzed. The animation lasts 105s and consists of seven consecutive back and forth walking motions, separated by 180° turns. The turns take place at approximately the following moments(s): 12.2 - 16.3, 27.7 - 32.5, 43.5 - 47.9, 59.8 - 63.5, 74.9 - 79.1, 90.6 - 94.6.

Figure 6 represents the graphs for the difference between joint strength every two seconds, *incremental*. The first row shows the graphs for the left hip and left knee DOFs corresponding to the rotation around the lateral axis. The second row for the left shoulder DOF corresponding to the rotation around the anterior axis and for the left elbow DOF corresponding to the rotation around the lateral axis.

Compared to the jumps, which displayed strong peaks, the leg joints show a relatively constant variation. It can be noticed in the arm joints that, while during walking, the fatigue does not vary greatly, the variation

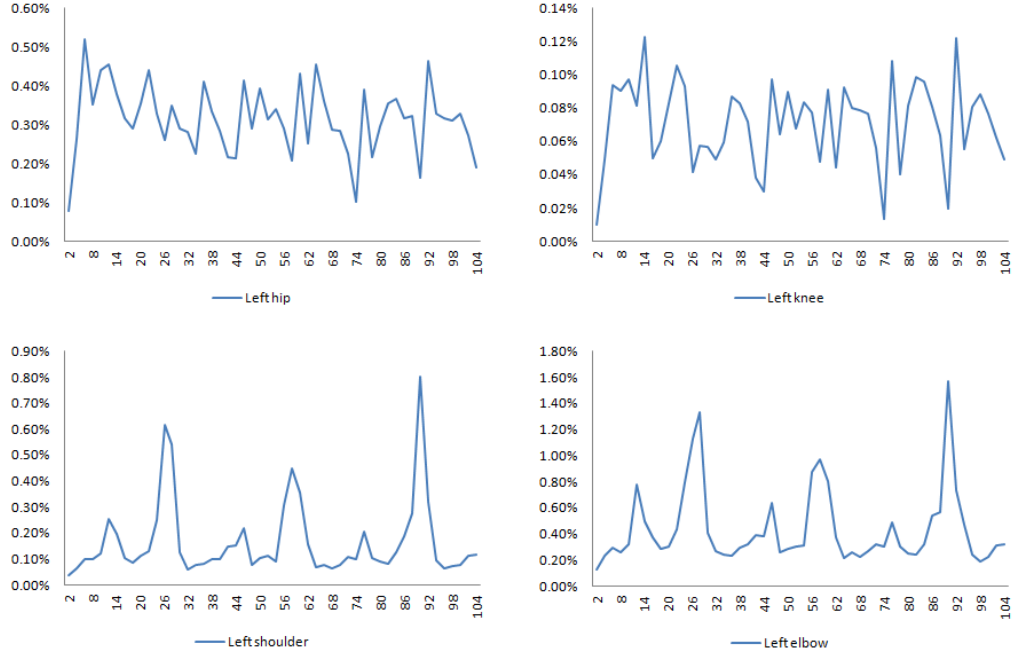


Figure 6: Difference between joint strength every two seconds for a walking sequence

at turns is clearly noticeable. The six turns that separate the seven walking sequences are visible in the second row of Figure 6 showing the difference between joint strength every two seconds for the arm joints.

Table 3: Normalized leg joints strength for a walking sequence

Time(s)	Left hip			Left knee		
	<i>current</i>	<i>incremental</i>	<i>relative</i>	<i>current</i>	<i>incremental</i>	<i>relative</i>
2	99.92%	0.08%	0.08%	99.99%	0.01%	0.01%
4	99.66%	0.26%	0.34%	99.94%	0.05%	0.06%
6	99.14%	0.52%	0.86%	99.85%	0.09%	0.15%
8	98.78%	0.35%	1.22%	99.76%	0.09%	0.24%
10	98.35%	0.44%	1.65%	99.66%	0.10%	0.34%
12	97.89%	0.46%	2.11%	99.58%	0.08%	0.42%
14	97.51%	0.38%	2.49%	99.46%	0.12%	0.54%
16	97.20%	0.32%	2.80%	99.41%	0.05%	0.59%
18	96.91%	0.29%	3.09%	99.35%	0.06%	0.65%
20	96.55%	0.36%	3.45%	99.26%	0.08%	0.74%
22	96.11%	0.44%	3.89%	99.16%	0.11%	0.84%
24	95.78%	0.33%	4.22%	99.06%	0.09%	0.94%
26	95.52%	0.26%	4.48%	99.02%	0.04%	0.98%
28	95.17%	0.35%	4.83%	98.96%	0.06%	1.04%
...	...	...	...	...	...	...
78	87.66%	0.22%	12.34%	97.28%	0.04%	2.72%
80	87.37%	0.30%	12.63%	97.20%	0.08%	2.80%
82	87.01%	0.36%	12.99%	97.10%	0.10%	2.90%
84	86.64%	0.37%	13.36%	97.00%	0.10%	3.00%
86	86.33%	0.32%	13.67%	96.92%	0.08%	3.08%
88	86.00%	0.32%	14.00%	96.86%	0.06%	3.14%
90	85.84%	0.16%	14.16%	96.84%	0.02%	3.16%
92	85.38%	0.46%	14.62%	96.72%	0.12%	3.28%
94	85.05%	0.33%	14.95%	96.66%	0.05%	3.34%
96	84.73%	0.32%	15.27%	96.58%	0.08%	3.42%
98	84.42%	0.31%	15.58%	96.49%	0.09%	3.51%
100	84.09%	0.33%	15.91%	96.42%	0.08%	3.58%
102	83.82%	0.27%	16.18%	96.36%	0.06%	3.64%
104	83.63%	0.19%	16.37%	96.31%	0.05%	3.69%

The fatigue evaluation for the same walking sequence (the first two and the last two walking cycles) is given in Tables 3 and 4. The tables show the normalized physical strength (*current*), the difference between the joint strength (*incremental*), and the difference between the joint strength and the maximum joint strength (*relative*) every two seconds for the left leg joints and the left arm joints respectively.

Table 4: Normalized arm joints strength for a walking sequence

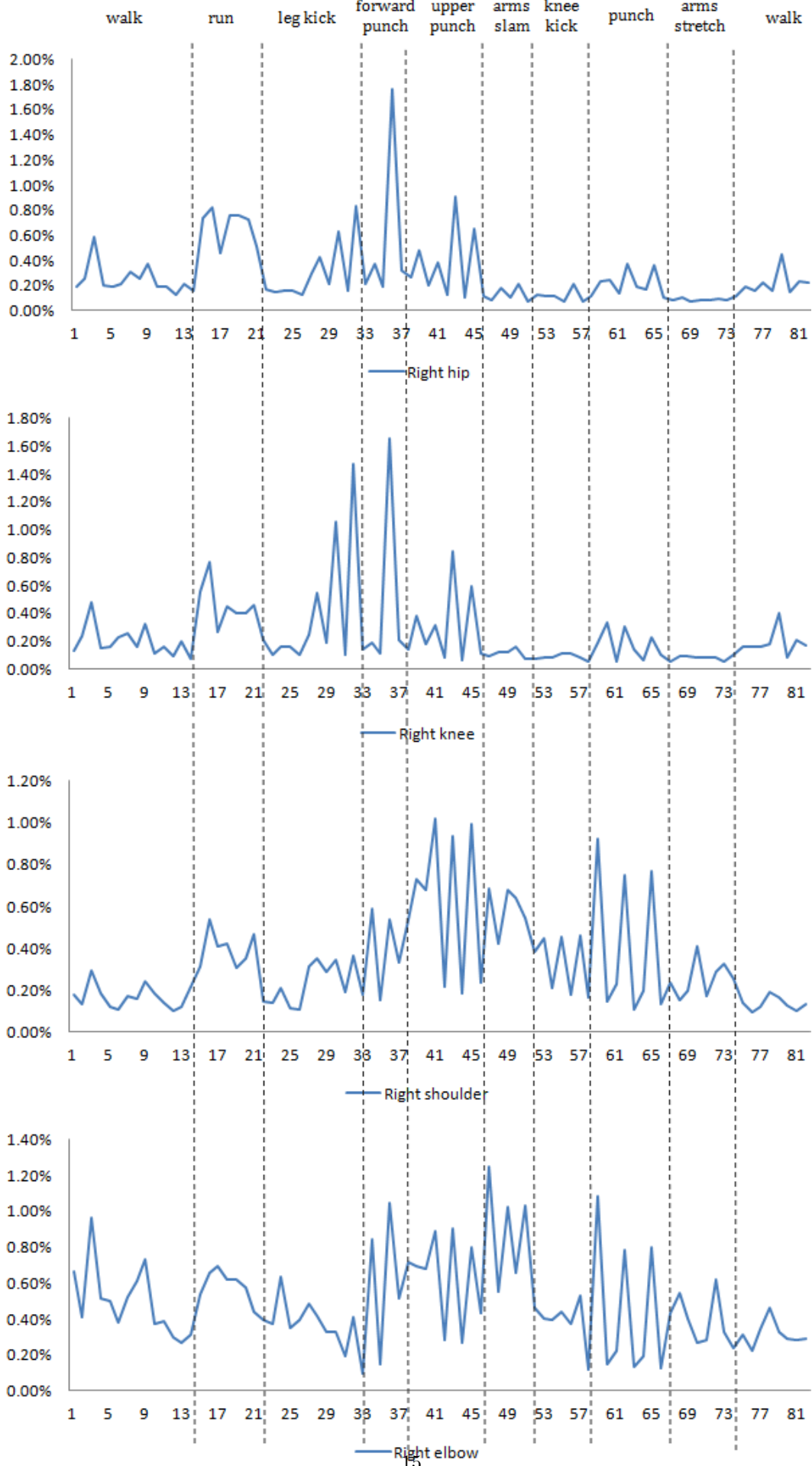
Time(s)	Left shoulder			Left elbow		
	<i>current</i>	<i>incremental</i>	<i>relative</i>	<i>current</i>	<i>incremental</i>	<i>relative</i>
2	99.96%	0.04%	0.04%	99.85%	0.13%	0.15%
4	99.89%	0.07%	0.11%	99.62%	0.23%	0.38%
6	99.80%	0.10%	0.20%	99.32%	0.30%	0.68%
8	99.69%	0.10%	0.31%	99.06%	0.26%	0.94%
10	99.57%	0.12%	0.43%	98.73%	0.32%	1.27%
12	99.32%	0.25%	0.68%	97.96%	0.78%	2.04%
14	99.12%	0.20%	0.88%	97.46%	0.50%	2.54%
16	99.02%	0.11%	0.98%	97.08%	0.38%	2.92%
18	98.93%	0.09%	1.07%	96.79%	0.29%	3.21%
20	98.82%	0.11%	1.18%	96.49%	0.30%	3.51%
22	98.69%	0.13%	1.31%	96.05%	0.44%	3.95%
24	98.44%	0.25%	1.56%	95.25%	0.80%	4.75%
26	97.82%	0.61%	2.18%	94.12%	1.13%	5.88%
28	97.28%	0.54%	2.72%	92.79%	1.33%	7.21%
...	...	...	...	...	...	...
78	93.76%	0.10%	6.24%	83.01%	0.30%	16.99%
80	93.67%	0.09%	6.33%	82.77%	0.25%	17.23%
82	93.59%	0.08%	6.41%	82.53%	0.24%	17.47%
84	93.46%	0.13%	6.54%	82.20%	0.32%	17.80%
86	93.27%	0.19%	6.73%	81.67%	0.54%	18.33%
88	93.00%	0.28%	7.00%	81.10%	0.56%	18.90%
90	92.19%	0.80%	7.81%	79.53%	1.57%	20.47%
92	91.87%	0.32%	8.13%	78.80%	0.73%	21.20%
94	91.78%	0.09%	8.22%	78.33%	0.47%	21.67%
96	91.72%	0.06%	8.28%	78.09%	0.24%	21.91%
98	91.64%	0.07%	8.36%	77.90%	0.19%	22.10%
100	91.57%	0.08%	8.43%	77.68%	0.22%	22.32%
102	91.45%	0.11%	8.55%	77.36%	0.32%	22.64%
104	91.34%	0.12%	8.66%	77.04%	0.32%	22.96%

Although the walking sequence and the jumps were performed by two different subjects, the results are clearly different, which makes a comparison plausible. It can be seen that, while the walking animation is approximately nine times longer than the jumps animation, the normalized physical strength drops at a much slower rate for all presented joints. This coincides with the fact that walking is a casual activity that does not consume much of one’s energy, while performing a set of jumps with the heels touching in mid-air is indeed an energy consuming activity.

The second column, the difference between joint strength, also shows much smaller numbers (under 1%) than the jumping animations. The normalized physical strength drops at most to 77.04% for the elbow joint during the entire walking sequence, while for the jumping sequence, the normalized physical strength drops to 63.63% for the same joint in a much shorter period of time.

**Acrobatics** Lastly, this chapter shows the results on an acrobatics sequence performed by a third subject. The animation lasts 82s and consists of several activities, as depicted in Figure 7. The DOFs for which the difference in joint strength is plotted are: the rotation around the lateral axis for the right hip, right knee and right elbow respectively, and the rotation around the anterior axis for the right shoulder joint. The graphs show how the effort exerted by a joint increases or decreases, according to the performed activity. For example, the difference in joint strength in the leg is visibly higher for running than for walking, and even higher for the leg kick. Also, for the arm, the punches inflict a higher decay rate of the current joint strength than walking or stretching.

Figure 7: Difference between joint strength every second for a mixed actions sequence





## 5 Conclusions

The main achievement of this project is putting together a number of different resources in a coherent way to obtain the fatigue evaluation at joint level. As the core pipeline now exists, it is possible to obtain a better fatigue evaluation, either by coming up with a more consistent motion capture dataset and the afferent information about the performer, either by improving the scaling method, or both.

Three motions were analyzed in Section 4. The first motion, a sequence of jumps, was chosen to show that the model indeed reflects an increased effort at the specific moments in time when the jumps take place. The second motion, a sequence of walking cycles, was discussed as walking is a common activity analyzed in computer animation. The third motion, a sequence of various sport activities was aimed to illustrate that the model confirms which body parts exert more effort depending on the type of activity.

The first motion displayed peaks of the difference in joint strength at the jumps and showed a relatively quick tiring rate. In comparison, the second motion, a steady walking sequence displayed relatively constant variation of the difference in joint strength for the leg joints and peaks of the difference in joint strength only for the arm joints at turns. Also, the tiring rate was much inferior to the jumping sequence, even during a period of time nine times longer.

The program can process multiple animation sequences in a fairly low amount of time and, depending on the purpose of the evaluation, different performances of the same motion can be compared, to see which inflicts more fatigue on separate joints, for example.

This fatigue model combined with a recovery model [Ma et al., 2010] could be applied in physics-based computer animation to limit the joint and muscle strength in time. Knowing the current exertable muscle force would prevent the character from performing otherwise implausible motions. The model however does not consider brain effort [Liu et al., 2002] and is based solely on the activity history of the joint or muscle. Therefore one cannot infer from the fatigue evaluation whether a subject performs in a way because they become tired or because they didn't feel motivated to perform better. The same reasoning would apply to motion editing considering fatigue, namely that the character would only display a constant voluntary brain effort. To exemplify, the model would probably not be suitable to animate athletes.

**Advantages** The fatigue model proposed by [Ma et al., 2009] is intuitive to understand, due to the fact that it is based on the way in which humans perceive fatigue on their own bodies (see Section 2). Another advantage, and the main reason for which the model was chosen as the topic of this project, is that it is implementable with existing resources. Although putting together a consistent pipeline which reunites different programming libraries, a motion capture dataset available online, and two models from literature for the inertial properties was a delicate task, the fatigue model itself was easy to implement.

**Drawbacks** Scaling body segment inertial parameters is a sensitive issue and much work is carried specifically on this problem (e.g. [Dumas et al., 2007]). To obtain an accurate scaling, both precise measurements (mass, length of body segments) of the motion capture performer and consistent segmentation with literature resources are required. Despite efforts to ensure consistency and precision, scaling in this project is merely an approximation, as data was collected from different resources.

In this project, the maximum joint strength was obtained by scanning all the torques that were available for a motion capture performer and is subject to the limitation of the motion capture dataset. Some accuracy is also lost through the modification of the skeleton hierarchy which inherently leads to some artifacts in motion. Accurate MVC measurement requires an experimental setup (e.g. the one used in [Ma et al., 2012] made of a dynamometer, a weight to be grabbed which was customized to fit the task of interest, a metronome to measure the sample times of the motion and a support to maintain the posture and measure the torques). The fact that the authors studied only one joint (the elbow) for only one person, shows that this procedure is quite complicated and needs to be customized for a particular task.

**Future work** [Ma et al., 2012] took an important step in the direction of validating their model in the case of dynamic motions. They investigated the model at joint level and used the robotic dynamic model to express the joint torque as depending on the angle, velocity, acceleration and the internal/external load. Motivated by the fact that two muscle groups create a joint torque, the fatigue rate parameter  $k$  (so far considered constant) was studied for both the agonist and antagonist muscles. Precise values were hard

to find or to generalize, but a valuable insight was gained in how the model can be perfected for dynamic situations.

## **Acknowledgement**

The data used in this project was obtained from [mocap.cs.cmu.edu](http://mocap.cs.cmu.edu). The database was created with funding from NSF EIA-0196217.

## A BVH file format

This section continues the explanations from [BVH file format](#). The header of the hierarchy section is the keyword HIERARCHY. The following line starts with the keyword ROOT and the name of the bone that is the root of the skeletal hierarchy. Then, the character structure is defined recursively, with each child described within curly braces inside its parent bone.

Every child definition starts with the keyword JOINT, followed by its name. Next, the translation of the origin with respect to the parents origin is given after the keyword OFFSET along the x, y and z-axis respectively. The CHANNELS define the degrees of freedom (DOFs) of the joint in the same order that they are given in the motion section of the file. End-effectors (bones with no children) are marked by the keywords *End Site*, and are described only by an OFFSET.

The header of the motion section is the keyword MOTION. This section contains the number of frames in the animation (preceded by the keyword *Frames*), frame rate (preceded by the keyword *Frame Time*) and the channel data for each frame and each DOF in the exact order that was defined in the hierarchy section.

## B BVH file template

```
HIERARCHY
2  ROOT Hips
   {
4     OFFSET 0.00000 0.00000 0.00000
   CHANNELS 6 Xposition Yposition Zposition Zrotation Yrotation Xrotation
6     JOINT LeftUpLeg
   {
8         OFFSET 0.00000 0.00000 0.00000
   CHANNELS 3 Zrotation Yrotation Xrotation
10        JOINT LeftLeg
   {
12            OFFSET 0.00000 0.00000 0.00000
   CHANNELS 3 Zrotation Yrotation Xrotation
14            JOINT LeftFoot
   {
16                OFFSET 0.00000 0.00000 0.00000
   CHANNELS 3 Zrotation Yrotation Xrotation
18                JOINT LeftToeBase
   {
20                    OFFSET 0.00000 0.00000 0.00000
   CHANNELS 3 Zrotation Yrotation Xrotation
22                    End Site
   {
24                        OFFSET 0.00000 0.00000 0.00000
26                    }
28                }
30            }
32        }
34    }
36    JOINT RightUpLeg
   {
38        % similar to LeftUpLeg
40    }
42    JOINT LowerBack
   {
44        OFFSET 0.00000 0.00000 0.00000
   CHANNELS 3 Zrotation Yrotation Xrotation
46        JOINT Spine
   {
48            OFFSET 0.00000 0.00000 0.00000
   CHANNELS 3 Zrotation Yrotation Xrotation
50            JOINT Neck1
   {
52                OFFSET 0.00000 0.00000 0.00000
   CHANNELS 3 Zrotation Yrotation Xrotation
54                End Site
   {
56                    OFFSET 0.00000 0.00000 0.00000
58                }
59            }
60        }
61    }
62    JOINT LeftArm
   {
64        OFFSET 0.00000 0.00000 0.00000
   CHANNELS 3 Zrotation Yrotation Xrotation
66        JOINT LeftForeArm
```

```

60     {
61         OFFSET 0.00000 0.00000 0.00000
62         CHANNELS 3 Zrotation Yrotation Xrotation
63         JOINT LeftHand
64     {
65         OFFSET 0.00000 0.00000 0.00000
66         CHANNELS 3 Zrotation Yrotation Xrotation
67         JOINT LeftFingerBase
68     {
69         OFFSET 0.00000 0.00000 0.00000
70         CHANNELS 3 Zrotation Yrotation Xrotation
71         JOINT LeftHandIndex1
72     {
73         OFFSET 0.00000 0.00000 0.00000
74         CHANNELS 3 Zrotation Yrotation Xrotation
75         End Site
76     {
77         OFFSET 0.00000 0.00000 0.00000
78     }
79     }
80     }
81     JOINT LThumb
82     {
83         OFFSET 0.00000 0.00000 0.00000
84         CHANNELS 3 Zrotation Yrotation Xrotation
85         End Site
86     {
87         OFFSET 0.00000 0.00000 0.00000
88     }
89     }
90     }
91     }
92     }
93     JOINT RightArm
94     {
95         % similar to LeftArm
96     }
97     }
98     }
99     }
100 }
101 MOTION
102 Frames: 0
    Frame Time: .0083333

```

template.bvh

## C GEAR Inverse Dynamics

The GEAR library implements a linear-time hybrid dynamics algorithm developed by [Featherstone, 1987]. The hybrid dynamics algorithm is a generalized version of the traditional forward and inverse dynamics algorithms. The whole algorithm is explained in [Kim and Pollard, 2011]. The skeleton on which this algorithm is applied is an articulated rigid body system with a tree topology, with one of the bones virtually connected to the ground via a *root* joint.

Listing 3 selects the relevant inverse dynamics algorithm used to calculate the joint torques. The first loop updates kinematic information such as the global position and velocity of each bone. The second loop calculates torques on each joint.

```

1 for all bodies in order
  update homogeneous transform from parent coordinate frame  $\{\gamma(i)\}$  to body coordinate frame  $\{i\}$ :
   $T_{\gamma(i),i} = \text{function of } q_i$ 
3  update generalized velocity of body  $i$ , viewed in  $\{i\}$ :  $V_i = Ad_{T_{\gamma(i),i}^{-1}} V_{\gamma(i)} + S_i \dot{q}_i$ 
  calculate temporary variable:  $\eta_i = ad_{V_i} S_i \dot{q}_i + \dot{S}_i \dot{q}_i$ 
5  update component-wise time derivative of  $V_i$ :  $\dot{V}_i = Ad_{T_{\gamma(i),i}^{-1}} \dot{V}_{\gamma(i)} + S_i \ddot{q}_i + \eta_i$ 
7 for all bodies in reversed order
  update generalized force transmitted to body  $i$  from its parent through the connecting joint  $i$ ,
  viewed in  $\{i\}$ :  $F_i = \hat{J}_i \cdot \dot{V}_i - ad_{V_i}^* \cdot J_i V_i - F_i^{ext} + \sum_{k \in \mu(i)} Ad_{T_{i,k}^{-1}}^* F_k$ 
  update torque (or force) acting on joint  $i$ :  $\tau_i = S_i^T \cdot F_i$ 

```

Listing 3: Inverse dynamics algorithm implemented in void GSystem::calcInverseDynamics()

For more details about the notations in Listing 3 as well as about the algorithm itself, the reader is referred to [Kim and Pollard, 2011].

## D Application description

The application takes as input the BVH files grouped per subject in the *data\motion* folder and outputs the fatigue files in the *data\fatigue.info* folder. The fatigue files are numbered correspondingly to the animation that they are related to and placed in the subject's folder created at runtime. The fatigue files are text files and correspond to three categories: the joint torques at each frame<sup>1</sup> in the animation, an mvc file containing the maximum exerted torques for each DOF, and the actual fatigue files which contain the current joint strength with time, at a time interval which can be defined in the *fatigue.cpp* file. These numbers can then be used for processing. All the graphs presented in this report were obtained in MS Excel. The figures were captured from the GMOV animation viewer.

**Steps** Follow the steps below to run the application for a subject:

- a. Copy a folder corresponding to a subject (e.g. folder *86*) from the original *motion capture* folder to the *data\original* folder in the *BVHAdapter* project.
- b. Run the *BVHAdapter* project to obtain the modified BVH files in a folder located in *data\processed* (e.g. *data\processed\subject86*).
- c. Copy the folder with the modified BVH files in the *data\motion* folder of the *exp\_proj* project.
- d. Set the time step (this is set at one second by default) at which the results are written in the output files by modifying the value for *N* in *fatigue.cpp* and run the *exp\_proj* application.
- e. The output files are found in the corresponding folder from *data\fatigue.info* (e.g. *data\fatigue.info\subject86*).

---

<sup>1</sup>The simulation step is defined in the GMOV application, with a frame time of 0.03030s corresponding to the rendering frame rate of 33 fps, which is lower than the frequency at which the motion capture data was recorded, namely 120 fps.

## References

- Liang Ma, Damien Chablat, Fouad Bennis, and Wei Zhang. A new simple dynamic muscle fatigue model and its validation. *International Journal of Industrial Ergonomics*, 39(1):211 – 220, 2009.
- Liang Ma, Damien Chablat, Fouad Bennis, Wei Zhang, and François Guillaume. A new muscle fatigue and recovery model and its ergonomics application in human simulation. *Virtual and Physical Prototyping*, 5(3):123–137, 2010.
- OpemSim CMC tool. URL <http://simtk-confluence.stanford.edu:8080/display/OpenSim/How+CMC+Works>.
- CMU Graphics Lab Motion Capture Database. URL <http://mocap.cs.cmu.edu/>.
- Junggon Kim. GEAR (Geometric Engine for Articulated Rigid-body simulation), a. URL <http://www.cs.cmu.edu/~junggon/tools/gear.html>.
- Liang Ma, Damien Chablat, Fouad Bennis, Wei Zhang, Bo Hu, and François Guillaume. Fatigue evaluation in maintenance and assembly operations by digital human simulation in virtual environment. *Virtual Real.*, 15(1):55–68, March 2011a.
- Liang Ma, Damien Chablat, Fouad Bennis, Wei Zhang, Bo Hu, and François Guillaume. A novel approach for determining fatigue resistances of different muscle groups in static cases. *International Journal of Industrial Ergonomics*, 41(1):10–18, 2011b.
- Jouni Freund and Esa-Pekka Takala. A dynamic model of the forearm including fatigue. *Journal of Biomechanics*, 34(5):597 – 605, 2001.
- A.S. Wexler, J. Ding, and S.A. Binder-Macleod. A mathematical model that predicts skeletal muscle force. *Biomedical Engineering, IEEE Transactions on*, 44(5):337–348, 1997.
- J.Z. Liu, R.W. Brown, and G.H. Yue. A dynamical model of muscle activation, fatigue, and recovery. *Biophysical journal*, 82(5):2344–2359, 2002.
- Bruce Hahne. BVH conversions of the 2500-motion Carnegie-Mellon motion capture dataset: MotionBuilder-friendly version. 2008. URL <https://sites.google.com/a/cgspeed.com/cgspeed/motion-capture>.
- M. Meredith and S. Maddock. *Motion Capture File Formats Explained*. Department of Computer Science, University of Sheffield, 211 Portobello Road, Sheffield, S1 4DP.
- Junggon Kim. GMOV (A simple motion capture data viewer), b. URL <http://www.cs.cmu.edu/~junggon/tools/gmov.html>.
- Harry G. Armstrong Aerospace Medical Research Laboratory. Military male aviators. In *Anthropometry and mass distribution for human analogues*, volume 1. U.S. Army, Air Force, and Navy, March 1988.
- Opensim models. URL <http://simtk-confluence.stanford.edu:8080/display/OpenSim/OpenSim+Models>.
- Opensim. URL <https://simtk.org/home/opensim>.
- Marcin Kalicinski. RapidXml, 2009. URL <http://rapidxml.sourceforge.net/index.htm>.
- R. Dumas, L. Cheze, and J.P. Verriest. Adjustments to McConville et al. and Young et al. body segment inertial parameters. *Journal of biomechanics*, 40(3):543–553, 2007.
- R. Ma, D. Chablat, F. Bennis, and L. Ma. Human muscle fatigue model in dynamic motions. *Latest Advances in Robot Kinematics*, pages 349–356, 2012.
- R. Featherstone. *Robot dynamics algorithms*. Kluwer, 1987.
- Junggon Kim and Nancy S. Pollard. Fast simulation of skeleton-driven deformable body characters. *ACM Trans. Graph.*, 30(5):121:1–121:19, October 2011.